

PAPER • OPEN ACCESS

Optimization of Acid Orange II Degradation using $\text{Fe}_{3-x}\text{Mn}_x\text{O}_4$ Catalyst in UV assisted Fenton-like reaction

To cite this article: Elsabba Edwin *et al* 2019 *IOP Conf. Ser.: Mater. Sci. Eng.* **551** 012126

View the [article online](#) for updates and enhancements.

Optimization of Acid Orange II Degradation using $\text{Fe}_{3-x}\text{Mn}_x\text{O}_4$ Catalyst in UV assisted Fenton-like reaction

Elsabba Edwin¹, Nor Aida Zubir^{1,2*}, Mohamad Khairul Azam Selamat¹, Rasyidah Alrozi^{1,2}, Norhaslinda Nasuha^{1,2}, Hawaiah Imam Maarof^{2,3}

¹Faculty of Chemical Engineering, Universiti Teknologi MARA, Cawangan Pulau Pinang, 13500 Pulau Pinang, Malaysia

²Hybrid Nanomaterials, Interfaces & Simulation (HYMFAST), Faculty of Chemical Engineering, Universiti Teknologi MARA, Cawangan Pulau Pinang, 13500 Pulau Pinang, Malaysia

³Faculty of Chemical Engineering, Universiti Teknologi MARA, Shah Alam, Selangor, Malaysia

E-mail: noraida709@uitm.edu.my

Abstract. In this work, detailed investigation on the optimization of acid orange II (AOII) degradation using $\text{Fe}_{3-x}\text{Mn}_x\text{O}_4$ catalyst in UV assisted Fenton-like reaction was performed. The Central Composite Design (CCD) based on Response Surface Methodology (RSM) with four independent operational parameters (catalyst dosage, oxidant concentration, pH and UV irradiation) and one response (percentage of AOII removal) was applied for statistical and optimization analysis. The maximum AOII removal (~100%) was found at optimal conditions of 0.4 g/L catalyst dosage, 35 mM oxidant concentration, pH 2.6 and 3 x 9W UVC. Interestingly, validation of these optimal conditions was confirmed by the experimental findings of having less than 2% absolute deviation. Such findings confer that the derived empirical quadratic model was in good agreement with the experimental findings.

1. Introduction

Water pollution due to untreated dye-contaminated wastewater from textile dyeing industries posed a serious environmental problem. It has been estimated that 17~20% of industrial water pollution originated from textile [1] industries and approximately 15% of synthetic dyes are lost during the dyeing process [2] which subsequently turns to be dye-contaminated wastewater.

Treatment for wastewater that containing dye is considered to be one of the challenging areas in the environment fraternity. Physico-chemical treatments are effective in the removal of dye but high operational cost and production of secondary sludge limits their application [3,4]. Moreover, biological wastewater treatment is no longer suitable for the treatment of dye-contaminated wastewater due to the recalcitrant and inhibitory nature of these dyes. Hence, advanced oxidation process (AOPs) such as UV assisted Fenton-like reaction have end up as an increasing area of researchers interest for eliminating recalcitrant organic pollutants in wastewater because it is more efficient, non-selective and environmental friendly [5,6].

In UV assisted Fenton-like reaction, strong oxidizing agent of hydroxyl radicals ($\bullet\text{OH}$) [5,7] is produced in the reaction mixture of during catalysis. The strong oxidizing and reactivity of $\bullet\text{OH}$ radicals may turn a complex recalcitrant organic pollutant into harmless compounds such as carbon



dioxide (CO_2) and water (H_2O) [11]. For instance, the use of manganese substituted magnetite [8,9] as heterogeneous catalyst in UV assisted Fenton-like reaction have been highlighted recently due to its notable enhancement in both of catalytic performance and activity during catalysis.

In enhancing the overall catalytic performance of dye degradation in UV assisted Fenton-like reaction; multiple operational parameters are required to be optimized at the optimal values. In past, many researchers used one-factor-at-a-time (OFAT) approach [8-12] for such purposes. However, this approach possessed of several limitations such as i) unable to provide detailed interaction between operational parameters towards the responses, ii) requires numerous experimental runs and iii) time-consuming and costly. In circumventing these limitations, an interactive approach known as response surface methodology (RSM) has been introduced to facilitate the detailed global interactions between operational parameters in process optimization. Therefore, the present work focuses on the determination of optimal operational conditions particularly on acid orange II degradation using manganese substituted magnetite ($\text{Fe}_{3-x}\text{Mn}_x\text{O}_4$) catalyst in UV assisted Fenton-like reaction.

2. Methodology

2.1. Synthesis of manganese substituted magnetite ($\text{Fe}_{3-x}\text{Mn}_x\text{O}_4$) catalysts

The $\text{Fe}_{3-x}\text{Mn}_x\text{O}_4$ catalysts at x value of 0.3 were synthesized through precipitation-oxidation method. First, 40 mL of 0.05 M $\text{FeCl}_3 \cdot 6\text{H}_2\text{O}$ was mixed with 17.4 mL of 0.05 M MnCl_2 solution. The mixture was heated at 90°C using double boiling technique whilst continuously stirred for 10 min. Then, 1 M NaOH was added dropwise into the mixture until pH 10. The mixture was aged for another 30 min under constant stirring at 90°C . Then, the mixture was let to be cooled to room temperature. The resulting precipitates were centrifuged and washed several times with deionized water and dried at 90°C for 24h.

2.2. Optimization of UV assisted Fenton-like reaction using CCD-RSM

The photocatalytic activity of manganese substituted magnetite ($\text{Fe}_{3-x}\text{Mn}_x\text{O}_4$, $x=0.3$) catalysts were tested in heterogeneous UV assisted Fenton-like reaction using acid orange II (AOII) as the model pollutant. Central composite design (CCD) in RSM was applied as experimental design to determine the optimized operational parameters of UV assisted Fenton-like reaction. This experimental design was mathematically modelled and optimized by Design Expert 11.0.5.0 software (State-Ease, Inc.). A five-level-four-factor CCD was chosen with rotatable α value fixed at 2 [13].

Four operational parameters which also known as independent variables have been identified as the pH of solution, oxidant (H_2O_2) concentration, irradiation intensity and catalyst dosage. Detailed experimental range and level of each independent variable are presented in Table 1. The response variable of this experimental design was the percentage of AOII removal. A total number of 30 experimental runs were performed comprising 16 factorial points, 8 axial points and 6 replications at the center point. Experimental results were analyzed using analysis of variances (ANOVA) in interpreting the relationships between four independent variables and response variable of the experimental design. Data having p-value lower than 0.05 was considered statistically significant.

Table 1. Independent variables and coded levels for CCD-RSM.

Parameter	Unit	Code	- α	-1	0	+1	+ α
pH		A	2.0	2.5	3.0	3.5	4.0
Oxidant concentration	mM	B	5	15	25	35	45
Catalyst dosage	g/L	C	0.2	0.4	0.6	0.8	1.0
UV Irradiation intensity	Watts	D	0	1 x 9	2 x 9	3 x 9	4 x 9

The heterogeneous UV assisted Fenton-like reaction was performed using a custom made photoreactor set-up equipped with 4 x 9W UV-C lamp (Sankyo-GPX9, λ_{\max} of 257.3 nm). The reaction was initiated by switching on UV lamps after the addition of specific H_2O_2 concentration into 100 mL AOII solution consisting of specific catalyst dosage and pH accordance to the CCD-RSM experimental design (Table 1). The reaction was prolonged for 180 min at stirring rate of 200 rpm. Sampling solution was filtered through 0.2 μm syringe filters and the filtrates concentration were analyzed using portable spectrophotometer at λ_{\max} of 484 nm. The percentage of AOII/color removal can be calculated using Equation 1:

$$\text{Percentage of removal, } Y_1 (\%) = \frac{C_o - C_t}{C_o} \times 100 \quad (1)$$

where C_o is the initial concentration of AOII and C_t is the final AO7 concentration at 180 min of reaction.

3. Results and Discussion

3.1. ANOVA analysis

Table 2 summarizes the detailed set of CCD-RSM's experimental design together with its response variable (percentage of AOII/color removal). In this experimental design, the highest and lowest removal of AOII were found to be at 99.83% and 22.99%, respectively. The statistical analysis of variance (ANOVA) was performed based on the acquired response variable and presented in Table 3. The ANOVA analysis exhibited that the derived quadratic model was statistically significant with F-value and p-value of 30.40 and 0.0001, consecutively. The lack of fit p-values of 0.3914 implied that the lack of fit of this model was not significant relative to the pure error. The non-significant term indicated that the lack of fit is good and acceptable. Moreover, the model exhibits a decent regression coefficient (R^2) of 0.966 which suggested that the acquired experimental data were well-fitted to the derived quadratic model that could provide a good estimation of predicted response (percentage of AOII removal) as depicted in Fig. 1

Interestingly, small p-value of less than 0.05 were found in the operational parameter of pH (A), catalyst dosage (C) and UV irradiation (D) that signify these parameters to be significant in the regression of empirical quadratic model (equation 2). The coefficient with one coded factor represent the effect of the specific operational parameter, whilst the coefficients with two coded factors as well the second-order terms represent the direct interaction between operational parameters and its quadratic effect, respectively [14].

$$Y_1 (\%) = 47.69 - 21.06A - 0.19B - 8.72C + 2.98D + 0.05AB + 12.96AC - 0.06AD \\ + 0.95BC + 1.43BD - 0.49CD + 2.95A^2 - 1.68B^2 + 7.49C^2 + 0.85D^2 \quad (2)$$

Table-2. Experimental design of CCD-RSM with experimental values of AOII removal.

Run	Factor 1 A: pH	Factor 2 B: Oxidant concentration (mM)	Factor 3 C: Catalyst Dosage (g/L)	Factor 3 D: UV Radiation (W)	Response AOII/ Color Removal (%)
1	3.5	15	0.4	1	32.68
2	3.0	25	0.6	0	35.67
3	2.0	25	0.6	2	98.39
4	3.0	45	0.6	2	37.02
5	3.0	25	0.2	2	99.77
6	3.5	15	0.8	1	40.97

7	2.5	15	0.4	1	99.43
8	2.5	15	0.4	3	99.77
9	3.0	25	0.6	2	53.01
10	2.5	15	0.8	1	59.48
11	2.5	35	0.4	3	99.65
12	2.5	35	0.8	1	55.26
13	3.0	25	0.6	4	63.65
14	3.5	35	0.8	3	42.93
15	2.5	35	0.8	3	64.56
16	3.5	35	0.4	1	22.99
17	4.0	25	0.6	2	17.75
18	3.0	25	0.6	2	47.28
19	3.0	25	0.6	2	51.09
20	3.5	35	0.8	1	45.76
21	3.5	35	0.4	3	35.9
22	3.0	25	1.0	2	52.64
23	3.0	25	0.6	2	36.93
24	3.0	25	0.6	2	47.11
25	3.0	25	0.6	2	50.72
26	2.5	15	0.8	3	58.27
27	3.5	15	0.4	3	31.34
28	2.5	35	0.4	1	99.83
29	3.0	5	0.6	2	42.06
30	3.5	15	0.8	3	39.45

Table-3. ANOVA analysis for percentage of AOII removal (Y_1).

Source	Sum of Squares	df	Mean Square	F-value	p-value	
Model: Quadratic model	17312.00	14	1236.57	30.40	< 0.0001	Significant
A-pH	10647.52	1	10647.52	261.78	< 0.0001	
B-Oxidant concentration	0.8778	1	0.8778	0.0216	0.8852	
C-Catalyst Dosage	1823.00	1	1823.00	44.82	< 0.0001	
D-UV Irradiation Intensity	212.59	1	212.59	5.23	0.0372	
AB	0.0390	1	0.0390	0.0010	0.9757	
AC	2686.09	1	2686.09	66.04	< 0.0001	
AD	0.0663	1	0.0663	0.0016	0.9683	
BC	14.42	1	14.42	0.3546	0.5604	
BD	32.86	1	32.86	0.8079	0.3829	
CD	3.99	1	3.99	0.0981	0.7584	
A ²	239.19	1	239.19	5.88	0.0284	
B ²	77.37	1	77.37	1.90	0.1881	
C ²	1537.42	1	1537.42	37.80	< 0.0001	
D ²	19.84	1	19.84	0.4878	0.4956	
Lack of Fit	444.78	10	44.48	1.35	0.3914	Not significant

Source	Sum of Squares	df	Mean Square	F-value	p-value
Std. Dev.	6.38				
Regression Coefficient, R^2	0.9660				
Adjusted R^2	0.9342		Predicted R^2		0.8438

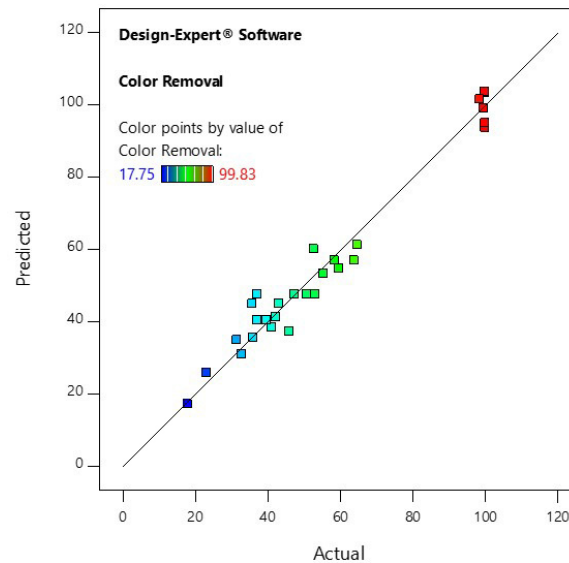


Figure 1. Plot of predicted vs. experimental values of AOII removal.

3.2. Interactions effect between operational parameters and optimization

Detailed interactions between these operational parameters was presented by the 3D response surface plots as shown in Figure 2. These plots reveal direct interaction effect between the operational parameter towards the percentage of AOII removal. Interestingly, significant interaction effect those operational parameters can be well observed between pH (A), catalyst dosage (C) and UV irradiation (D) rather than oxidant concentration (B) at the optimum conditions. For instance, high AOII removal can be attained at low pH range (Figure 2a), low catalyst dosage (Figure 2b) and high UV irradiation intensity (Figure 2 c,d) disregard to oxidant concentration (Figure 2a, Table 3 (p-value of 0.8852)). Similar observations were also reported in the previous work [11,15,16] related to degradation of dyes.

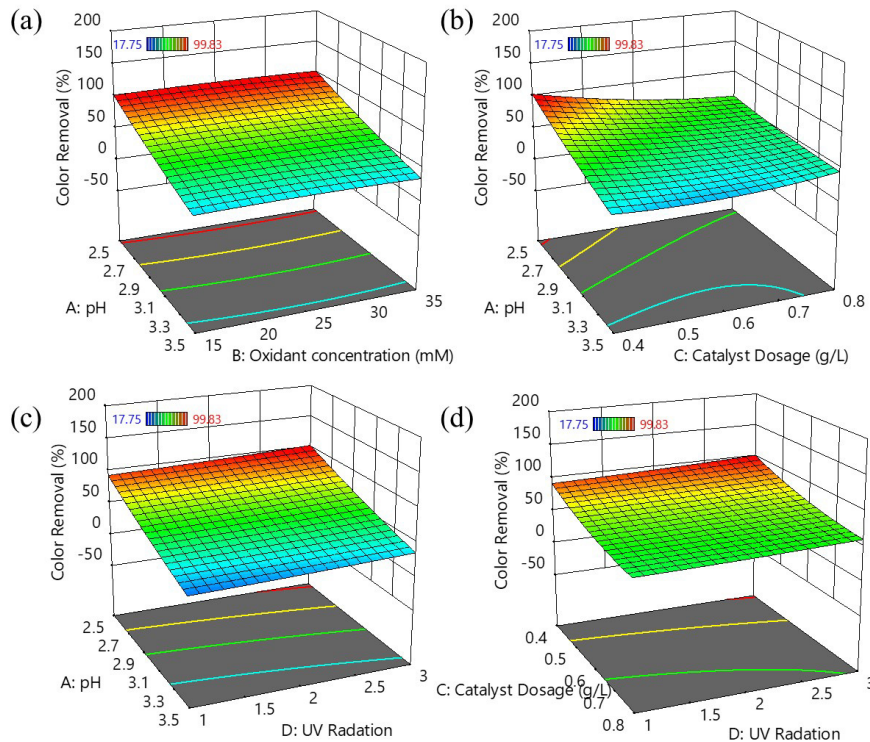


Figure 2. 3D response surface plots of (a) AB, (b) AC, (c) AD and (d) CD interaction effects towards AOII/ color removal (Y_1).

Such observations are in accordance with the proposed optimal operational conditions based on derived empirical quadratic model at desirability of 1. The maximum AOII (~100%) was anticipated at pH (A) solution of 2.6, 35 mM oxidant concentration (B), 0.4 g/L catalyst dosage (C) and 3 x 9W irradiation intensity (D). Validation of model reliability at these conditions were performed in duplicate runs. Interestingly, the percentage of AOII removal in both experimental runs were found to be at 99.78% and 97.45%. Small absolute deviation of less than 2% between the experimental and predicted values of AOII removal. Such findings confer that the derived empirical quadratic model was in good agreement with the experimental findings.

4. Conclusions

In conclusions, the optimal operational parameters for AOII degradation using $\text{Fe}_{3-x}\text{Mn}_x\text{O}_4$ catalyst were determined to be of solution pH (A) 2.6, oxidant concentration (B) 35mM, catalyst dosage (C) 0.4 g/L and UV irradiation (D) of 3 x 9W. At these conditions, the maximum predicted AOII removal was close to 100%. ANOVA analysis confers that interaction between pH, catalyst dosage and UV irradiation possessed significant influence towards the AOII removal during the reaction. In addition, the high regression coefficient value of 0.966 was in good agreement between the predicted and actual/experimental values of AOII removal. Hence, such findings present new insights into detailed global interactions between operational parameters for optimization of AOII degradation in UV assisted Fenton-like reaction particularly with utilization of $\text{Fe}_{3-x}\text{Co}_x\text{O}_4$ catalyst.

Acknowledgements

The authors gratefully acknowledged the Ministry of Higher Education Malaysia (MOHE) and Universiti Teknologi MARA (UiTM) for financial support under Fundamental Research Grant Scheme (600-IRMI/FRGS 5/3 (110/2016).

References

- [1] Kant R. 2012 *Natural Sci.* **4** 22
- [2] M.P. Prasad *et al* 2013 *J. Ecol. Environ. Sci.* **4** 4
- [3] Cao X. *et al.* 2018 *Chemosphere* **208** 219
- [4] Ramirez J.H. *et al* 2007 *Appl. Catal B* **75**, 312
- [5] Ahmed B *et al* 2011 *Ind. Eng. Chem. Res.* **50** 6673
- [6] Elboughdiri N *et al* 2015 *Adv. Chem. Eng. Sci. B*, **5** 111
- [7] Ahmadi M *et al* 2015, *Adv. Environ. Technol.* **2** 59
- [8] Zhong Y. *et al* 2014 *Appl. Catal B*, **150** 612
- [9] Liang X. *et al* 2014 *J. Colloid Inter. Sci.*, **426** 181
- [10] Zhou L. *et al* 2018 *Appl. Catal. B*, **237** 1160
- [11] Palas B *et al* 2016 *J. Photochem. Photobiol. A Chem.* **324** 165
- [12] Ramirez J.H. *et al* 2005 *Catal Today*, **107** 68
- [13] Bezerra M.A. *et al* 2008 *Talanta*. **76** 965
- [14] Abdullah N.H. *et al* 2018 *Mater. Today Proceed*, **5** 21956
- [15] Wei G.T *et al* 2012 *Catal. Commun.* **17** 184
- [16] Azami M *et al* 2012 *J. Serbian Chem. Soc.* **77** 235